

Fabrication and optical characterization of suspended 2D membranes for electromechanics

David Northeast* and Robert G. Knobel†

*Department of Physics,
Engineering Physics and Astronomy, Queen's University*

We report on a method for fabricating electromechanical structures using two-dimensional crystal materials and an all-resist process. Graphene and NbSe₂ are used as the mechanical elements in parallel plate capacitor elements with several microns of suspended diameters. The optical cavity formed from the membrane/air/metal structures enables a quick method to measure the number of layers and the gap separation using comparisons between the expected colour and optical microscope images.

I. MOTIVATION

Suspended membranes of graphene and other molecular membrane materials like transition metal dichalcogenides (TMDs) or hexagonal boron nitride (HBN) are, in many ways, ideal nanomechanical systems. Graphene exhibits high in-plane Young's modulus [1], high electron mobility down to a single layer of atoms [2], strain tunability of mechanical resonance [3], and the ability to be integrated with top-down lithographic processing. HBN and TMDs broaden the range of electrical parameters available in the mechanical material, enabling access to semiconducting, insulating, metallic, and superconducting materials for optical or electrical coupling in the design of devices or experiments [4, 5].

There are numerous applications for graphene and other thin membrane crystals in electromechanical and optomechanical systems, including as sensors [6] of force, strain, or mass. A local gate would allow the fabrication of membrane mechanical switches [7, 8] compatible with CMOS logic voltages, potentially increasing the switching speed and lowering energy loss [9]. Their low area mass can allow an enhancement of the response to radiation pressure forces in Fabry-Pérot cavity experiments, leading to new possibilities for transducers between optical and microwave photons [10] or between photons and phonons of different energies [11].

Several experiments have used graphene or TMD membranes as the mechanical element in experiments exploring the quantum regime of mechanical systems [12–15]. A suspended membrane of graphene over a metal electrode forms a vacuum gap capacitor whose capacitance varies as the membrane vibrates. Embedding this capacitor in a superconducting microwave electromagnetic resonator allows the electromagnetic resonance to be modified by the mechanical motion, introducing a strong electro-mechanical coupling. Bulk metallic membranes in such a system have proven to be a rich environment for probing the quantum regime of mechanical systems [16].

By using 2D membranes, the zero-point motion of the mechanical resonator can be made larger than for bulk devices and the quantum regime can be more accessible, provided the system loss remains low. To date the graphene-based experiments have been limited by the electrical loss in the material, so we are working to embed superconducting NbSe₂ membranes in such a device.

Fabricating mechanical systems using 2D crystal materials can be a difficult manufacturing challenge. The flexible membrane must be supported during processing, but this support must be removed to allow the suspension, all while keeping incompatible chemicals and processes away from the fragile membrane. Suspended graphene or TMD devices have been used in electromechanical resonators with global gates [3] [5], however these devices have limitations compared to locally gated devices. Suspended structures using 2D materials and local electrodes have been made by placing the membrane last over a surface with the electrode lowered by the intended gap distance [12, 13], however more complicated integration will require processing after the membrane has been placed. In this work we introduce a novel fabrication process where a 2D membrane is integrated into a superconducting coplanar circuit using resists for sacrificial layers and compatible chemicals for further processing.

In fabricating these devices, we required a quick, non-destructive method to characterize the thickness and suspended height of the membranes. In this work we introduce a generalization of the commonly used technique of examining thin layers on a known thickness of SiO₂ over silicon [2, 17], where thin film interference increases the graphene contrast. We extended this to allowed for the variation in gap thickness – the distance between the 2D crystal and an electrode metal layer underneath – to estimate the amount of out-of-plane height variation due to sagging or rippling in thin membranes. Here we use a colour camera with a white light source in a microscope operated in reflection mode and compare the resulting images with theoretical predictions based on Fresnel equations. This method avoids more complex optical or scanning probe measurements since simple microscope images can be used to acquire this information.

* david.northeast@queensu.ca

† knobel@queensu.ca

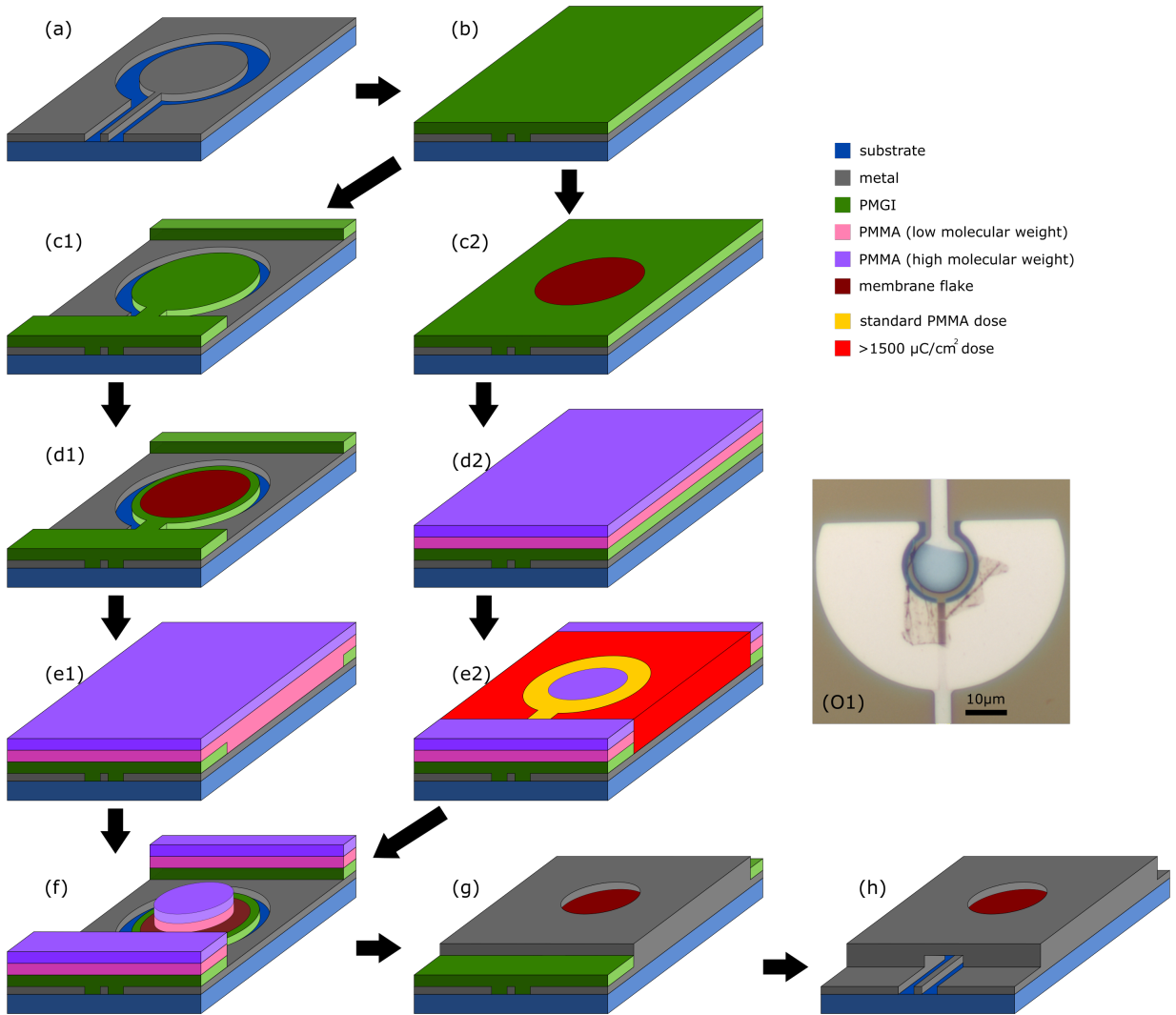


FIG. 1. The lithographic process to fabricate the suspended membrane structures starts with (a) a metallic structure on a substrate that is then (b) coated in PMGI. There are two variants to proceed. The first has the device patterned with e-beam lithography (c1) to open clamp windows to the metal. A 2D crystal membrane is placed over the resist-covered electrode (d1) and the chip is spin coated with (e1) two molecular weights of PMMA. This allows e-beam lithography to define clamping areas (f) for metal evaporation and lift off (g). The membrane is left freely suspended above the electrode by dissolving the PMGI in *n*-methyl-2-pyrrolidone and critical point drying (h). The second method has the membrane placed on the PMGI on step (c2), and the sample coated in two molecular weights of PMMA (d2). Step (e2) is a standard electron dose to pattern metal clamping areas for the membrane, and a high dose to pattern both the PMMA and PMGI following the process developed by Cui et al. [18]. Both processes are identical between steps (f)-(h). Image (O1) shows a stamped graphene membrane as in (d1).

II. METHODS AND PROCEDURES

Samples are prepared using exfoliated membranes of graphene or 2H-NbSe₂ taken from bulk crystals, thinned by several rounds of cleavage between two pieces of Nitto tape (SPV224). The thinned membranes are placed on polydimethylsiloxane (PDMS) sheets on a glass slide. A high magnification microscope is used to locate even-coloured crystals that appear thin and unfolded by optical contrast and have a suitable area for the electromechanical design. The glass slide is held by a modified photomask holder to allow the use of a mask aligner to

position the flake accurately to micron precision. This transfer method is adapted from the method reported by Castellanos-Gomez et al. [19].

A lumped-element *LC* circuit coupled to a co-planar waveguide was created on a highly resistive oxidized silicon wafer using photolithography and electron-beam evaporation of aluminum. For a nominally 100 nm separation of the membrane from the underlying aluminum electrode the *LC* resonant frequency is predicted to be 5 GHz, and vibration of the NbSe₂ membrane will change this with an estimated $\frac{\partial\omega}{\partial z} = 2\pi \times 5$ MHz/nm. A circular aluminum layer serves as the electrode underneath the

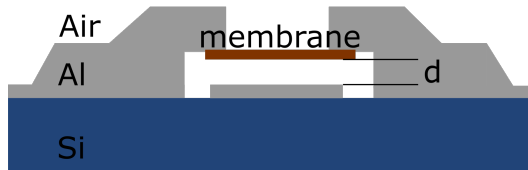


FIG. 2. Cross-sectional view of a finished device. The separation d is nominally set by the sacrificial resist thickness.

membrane and is the location over which the membrane is placed. Placement is achieved by using a mask aligner to make contact with the chip then slowly withdrawing, causing the PDMS to release the membrane.

The lithography process is shown schematically in Fig. 1. The process has two variations, and is based on resist research [18] into selectively changing the solvent compatibility of polymethylglutarimide (PMGI) resist based on electron beam dose. In both processes, a sacrificial layer (PMGI) coats the bottom layer of metal (Fig. 1(b)).

The first method has the PMGI layer patterned with a standard dose ($\sim 300 \mu\text{C}/\text{cm}^2$) and developed in AZ developer. This patterning opens via windows into the bottom metal layer but leaves the electrode covered in resist (Fig. 1(c1)). It is at this point that the membrane is stamped onto the chip (Fig. 1(d1)), then a bilayer of polymethyl methacrylate (PMMA) is spin coated onto the sample (Fig. 1(e1)). The bilayer typically consists of 950k molecular weight over 495k molecular weight PMMA that allows for an undercut profile and clean metal lift off (Fig. 1(f)-(g)). Figure 1(O1) is an optical image of a graphene membrane placed on PMGI, representing the step of Fig. 1(c1).

The second method has the 2D crystal placed at step Fig. 1(c2), then the two layers of PMMA are coated on top (Fig. 1(d2)). The PMMA can be patterned with an electron beam dose of $\sim 300 \mu\text{C}/\text{cm}^2$ (low dose) and developed in a solution of methyl isobutyl ketone (MIBK)/isopropyl alcohol (IPA) (1:3 ratio). At this dose, the PMGI will be unaffected and remain as a support for the membrane. If the applied dose is increased to $\sim 1500 \mu\text{C}/\text{cm}^2$ (high dose), the PMGI also becomes soluble in the MIBK/IPA mixture. This allows a low dose to define metal clamping structures over the membrane, then a high dose can be used to remove areas of developed PMGI where metal contacts are needed between top and bottom metal layers (Fig. 1(e2)). Steps Fig. 1(f)-(g) are identical with the first method.

The sacrificial PMGI layer under the membrane can be removed in two ways. In the first, all of the PMGI on the sample can be dissolved in *n*-methyl-2-pyrrolidone (NMP). The sample is placed into a beaker, then the NMP can be slowly replaced with acetone, which is then replaced with IPA. The second method makes use of either an electron beam dose, or deep UV exposure of the

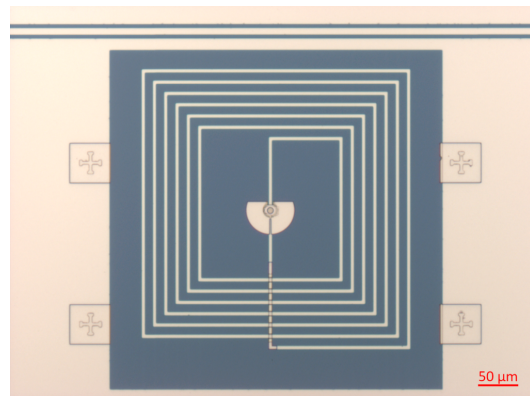


FIG. 3. A completed device, showing a spiral inductor coupled to a transmission line (top). A NbSe_2 membrane is placed over an electrode at the centre and air bridges connect the inner electrode to the outer loop.

PMGI resist under the membrane. This will allow the membrane to be removed by submerging the sample into a beaker of AZ developer, which is slowly replaced by deionized water, then IPA. In both cases, the sample undergoes critical point drying in CO_2 .

This process also allows for the formation of air bridge structures to connect only where desired to the bottom metal layer. This can be seen in Fig. 3 and Fig 1(O2), where air bridges of aluminum help connect the inner portion of a spiral inductor to the outer portion.

III. RESULTS

A. Interferometric colour analysis

The colour of the membrane, as seen from top down on the sample, is a function of the optical and geometric properties of the MEMS structure. If the complex refractive indices (given by $\underline{n}(\omega) = n(\omega) + i\kappa(\omega)$) and the gap thickness, d , are known, it can allow a quick and non-contact means to determine the number of membrane layers. If the membrane has some curvature indicating a change in the gap distance, which typically occurs with low layer numbers, this can also be estimated by colour variations.

Considering top-down illumination on the stack of materials seen in Fig. 2 and using the Fresnel equations on the layers, it is possible to calculate the total transmission and reflection. A wave travelling forward in the $x-z$ plane, in a material of thickness t_N with refractive index \tilde{n} , has a wavevector given by $\vec{k}_{f,i} = \frac{2\pi\tilde{n}_i}{\lambda_0} (\hat{z} \cos \theta + \hat{x} \sin \theta)$, at an angle θ from the normal. The total reflection (r) and transmission (t) from the stack can be related by

$$\begin{bmatrix} 1 \\ r \end{bmatrix} = \tilde{M} \begin{bmatrix} t \\ 0 \end{bmatrix}, \quad (1)$$

with \widetilde{M} given by

$$\widetilde{M} = \begin{bmatrix} 1 & r_{0,1} \\ r_{0,1} & 1 \end{bmatrix} M_1 M_2 \cdots M_{N-1}. \quad (2)$$

For each of the N layers of the stack, we have the M_N matrices

$$M_N = \begin{bmatrix} e^{-it_N k_z} & 0 \\ 0 & 0 \end{bmatrix} \begin{bmatrix} 1 & r_{N,N+1} \\ r_{N,N+1} & 1 \end{bmatrix} \frac{1}{t_{N,N+1}}. \quad (3)$$

In this, k_z , is the \hat{z} -component of $\vec{k}_{f,i}$. Calculating the total transmission and reflection through a layer of materials requires knowledge of the complex refractive indices and thicknesses of the materials. Over the visible range, the complex refractive indices of aluminum [20], graphene [17], and NbSe₂ [21] can be well characterized.

The changing contrast for different layers over a Si/SiO₂ substrate has been used since the discovery of graphene [2, 17]. Measuring the reflectivity at multiple wavelengths would allow for both the membrane thickness and air gap to be determined. This varying reflectivity manifests as different colours when observed with white light and either by eye or with a colour camera. We use a simulation program written in Python based on the *tmm* [22] package to calculate reflectances over the optical spectrum. The Python package *ColorPy* [23] allows us to simulate the apparent colour of the stack, and to compare both qualitatively and quantitatively to the fabricated devices.

A stack consists of a semi-infinite air layer above the membrane, then an air-filled gap, then a semi-infinite aluminum layer. Fig. 4(a) and 4(b) are plots showing the expected colours as the gap d and number of layers m are changed. There are periodic changes in expected colour as either number of layers or the gap distance are changed. Distinctions can be made due to a change in the lightness of the as well. At larger m (not shown in plots), the colour variation ceases as the material reaches the colour of the bulk material.

We extract the number of layers and gap from the colours when compared to digital microscope images of devices. We use the International Commission on Illumination's (CIE) D65 illuminant in the simulation. This is a white daylight illuminant that we compare with images taken with a Carl Zeiss Axio Imager A1m. Care is taken to colour balance the microscope camera against an unfocused image on white paper. In order to compare colours, we make use of the CIE colour difference function (CIEDE2000 implementation [24]), typically noted as ΔE . For ΔE , the 24 bit (RGB) pixel values are converted from this colour space to one based on lightness (L), red-green opponent colours (a) and blue-yellow opponent colours (b), called the Lab colour space, which is required for ΔE comparisons.

Fig. 5 shows some examples of devices made from graphene or NbSe₂. Comparing the colours of the membranes in optical photos with the simulation results in Fig. 4(a) and 4(b), it is possible to extract estimates for the number of crystal layers and the gap separation.

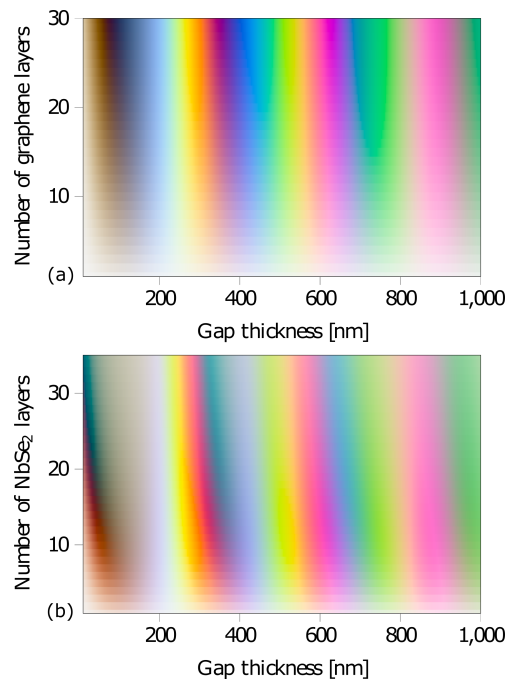


FIG. 4. Simulation of colour, as viewed from above, of a graphene/air/aluminum stack (a) and NbSe₂/air/aluminum stack (b). The colour is a function of both the number of crystal layers and gap distance, d .

The determination of the number of membrane layers and gap thickness can be found by routines that minimize the Fresnel equation and colour comparison functions. By taking a small section of an optical membrane photo, the average colour and standard deviation of the RGB values can be calculated. The periodicity of the interference requires that an educated guess be used to calculate the colours of a given number of layers (of the membrane in question) and gap separation. When this simulated colour is known, it can be compared to the average colour of the small section of image, by way of ΔE comparison. Minimization is done through an optimization routine where the derivative or second derivative need not be specified. In this work, the Nelder-Mead method is used to minimize, and does not require constraints. For problems where constraints are preferable, an alternative is the constrained optimization by linear approximation (COBYLA) method, which also does not require derivative functions. Solutions to the number of layers were made continuous for these calculations, with discretization possible afterwards.

Breaking up an optical image into a series of smaller rectangular images, it is possible to get estimates of the number of membrane layers and the gap distance simultaneously in the suspended area. Applying this along the diameter of the image (red rectangles in Fig. 5) provides an effective line cut, which can be seen in Figures 5(a2), 5(b2), 5(c2), and 5(d2). Device Fig. 5(a1) varies in membrane number over the suspended area, with a variation in height of 40 nm across the diameter.

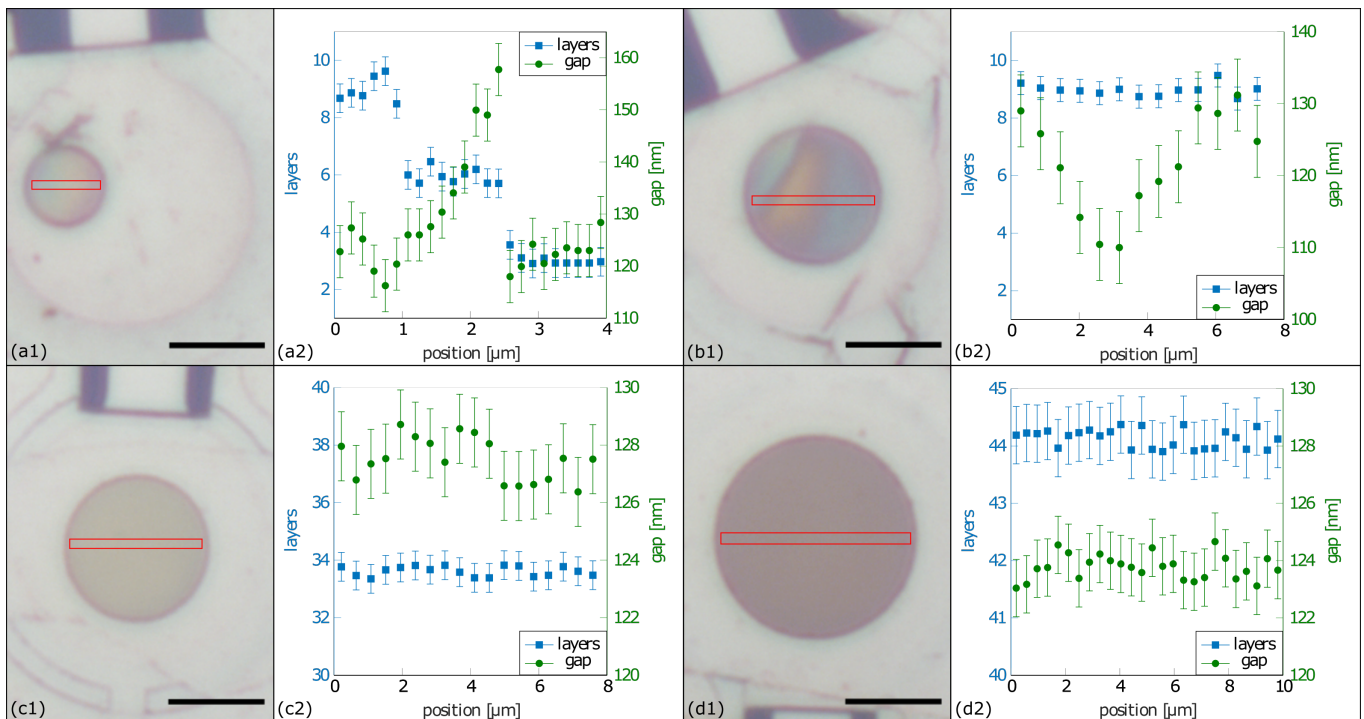


FIG. 5. Optical images of manufactured devices and cross section plots of the number of membrane layers and gap distance. Figure (a1) and (b1) are devices fabricated with graphene membranes, and Figures (c1) and (d1) are NbSe₂ membranes. The red rectangles in the circular membranes indicate the areas used in the cross sectional plots (with (a2) corresponding to the cross section of (a1), and so on). The plots show estimates of the number of membrane layers and the gap thickness at positions along the greater length of the red rectangles. Black scale bars in the optical images indicate a distance of 5 μm .

The other graphene sample, device Fig. 5(b1) appears to be a constant 9.0 ± 0.4 membrane layers thick, with a noticeable 20 nm of sagging over the circle. The NbSe₂ samples were thicker, with a constant gap distance as expected of their even colour. Sample Fig. 5(c1) was determined to be 33.0 ± 1.4 layers with a gap of 126.0 ± 2.2 nm. Fig. 5(d1) is 44.0 ± 0.9 layers with a gap of 123.1 ± 3.0 nm. Uncertainties in these values were determined through the standard deviation of the colour in the images used in the calculations. The colours deviating from the average can also be used to find the optimal solutions and provide a bounds of the uncertainty.

IV. SUMMARY

We have shown a fabrication technique to create electromechanical devices using exfoliated crystal materials. The technique uses exfoliated membrane crystals that are aligned over an area coated in PMGI resist. Circular membrane sections with diameters of over 10 μm can be released, provided quality crystal areas can be found to place over the intended location. The process uses a solvent release that avoids harsher techniques like hydrofluoric acid or reactive ion etching. Colours produced by optical interference, when observing the devices from below, can be used as a comparison with theory to estimate membrane thickness or surface curvature.

-
- [1] M. Poot and H. van der Zant, *Physics Reports* **511**, 273 (2012).
 [2] K. S. Novoselov, A. K. Geim, S. V. Morozov, D. Jiang, Y. Zhang, S. V. Dubonos, I. V. Grigorieva, and A. A. Firsov, *Science* **306**, 666 (2004).
 [3] C. Chen, S. Rosenblatt, K. I. Bolotin, W. Kalb, P. Kim, I. Kymissis, H. L. Stormer, T. F. Heinz, and J. Hone, *Nature Nanotechnology* **4**, 861 (2009).
 [4] B. Radisavljevic, A. Radenovic, J. Brivio, V. Giacometti, and A. Kis, *Nature Nanotechnology* **6**, 147 (2011).
 [5] S. Sengupta, H. S. Solanki, V. Singh, S. Dhara, and M. M. Deshmukh, *Physical Review B* **82**, 155432 (2010).
 [6] P. Weber, J. Güttinger, A. Noury, J. Vergara-Cruz, and A. Bachtold, *Nature Communications* **7**, 12496 (2016).
 [7] M. Nagase, H. Hibino, H. Kageshima, and H. Yamaguchi, *Applied Physics Express* **6**, 055101 (2013).
 [8] M. Dragoman, D. Dragoman, F. Coccetti, R. Plana, and A. A. Muller, *Journal of Applied Physics* **105**, 054309 (2009).

- [9] J. Sun, M. Muruganathan, N. Kanetake, and H. Mizuta, *Micromachines* **7**, 124 (2016).
- [10] T. Bagci, A. Simonsen, S. Schmid, L. G. Villanueva, E. Zeuthen, J. Appel, J. M. Taylor, A. Sørensen, K. Usami, A. Schliesser, and E. K. Polzik, *Nature* **507**, 81 (2014).
- [11] R. De Alba, F. Massel, I. R. Storch, T. S. Abhilash, A. Hui, P. L. McEuen, H. G. Craighead, and J. M. Parpia, *Nature Nanotechnology* **11**, 741 (2016).
- [12] P. Weber, J. Güttinger, I. Tsioutsios, D. E. Chang, and A. Bachtold, *Nano Letters* **14**, 2854 (2014).
- [13] V. Singh, S. J. Bosman, B. H. Schneider, Y. M. Blanter, A. Castellanos-Gomez, and G. A. Steele, *Nature Nanotechnology* **9**, 820 (2014).
- [14] X. Song, M. Oksanen, J. Li, P. J. Hakonen, and M. A. Sillanpää, *Physical Review Letters* **113**, 027404 (2014).
- [15] M. Will, M. Hamer, M. Müller, A. Noury, P. Weber, A. Bachtold, R. V. Gorbachev, C. Stampfer, and J. Güttinger, *Nano Letters* , 5950 (2017).
- [16] J. D. Teufel, T. Donner, D. Li, J. W. Harlow, M. S. Allman, A. J. Sirois, J. D. Whittaker, K. W. Lehnert, and R. W. Simmonds, *Nature* **475**, 359 (2011).
- [17] P. Blake and E. W. Hill, *Applied Physics Letters* **91**, 063124 (2007).
- [18] B. Cui and T. Veres, *Microelectronic Engineering* **85**, 810 (2008).
- [19] A. Castellanos-Gomez, M. Buscema, R. Molenaar, V. Singh, L. Janssen, H. S. J. van der Zant, and G. A. Steele, *2D Materials* **1**, 011002 (2014).
- [20] A. D. Rakić, *Applied Optics* **34**, 4755 (1995).
- [21] A. R. Beal, H. P. Hughes, and W. Y. Liang, *Journal of Physics C: Solid State Physics* **8**, 4236 (1975).
- [22] S. J. Byrnes, *arXiv* **30**, 21 (2016).
- [23] M. Kness, “colorpy 0.1.1,” <https://pypi.python.org/pypi/colorpy> (27 Aug. 2012).
- [24] G. Sharma, W. Wu, and E. N. Dalal, *Color research and application* **30**, 21 (2005).